

Regulation and Levels of the Thylakoid K^+/H^+ Antiporter KEA3 Shape the Dynamic Response of Photosynthesis in Fluctuating Light

Ute Armbruster^{1,2,3,*}, Lauriebeth Leonelli¹, Viviana Correa Galvis³, Deserah Strand³, Erica H. Quinn¹, Martin C. Jonikas² and Krishna K. Niyogi^{1,4}

¹Howard Hughes Medical Institute, Department of Plant and Microbial Biology, University of California, Berkeley, CA 94720, USA

²Carnegie Institution for Science, Department of Plant Biology, Stanford, CA 94305, USA

³Max Planck Institute of Molecular Plant Physiology, Am Mühlenberg 1, D-14476 Potsdam, Germany

⁴Physical Biosciences Division, Lawrence Berkeley National Laboratory, Berkeley, CA 94720, USA

*Corresponding author: E-mail, ute.armbruster78@gmail.com

(Received December 18, 2015; Accepted April 24, 2016)

Crop canopies create environments of highly fluctuating light intensities. In such environments, photoprotective mechanisms and their relaxation kinetics have been hypothesized to limit photosynthetic efficiency and therefore crop yield potential. Here, we show that overexpression of the Arabidopsis thylakoid K^+/H^+ antiporter KEA3 accelerates the relaxation of photoprotective energy-dependent quenching after transitions from high to low light in Arabidopsis and tobacco. This, in turn, enhances PSII quantum efficiency in both organisms, supporting that in wild-type plants, residual light energy quenching following a high to low light transition represents a limitation to photosynthetic efficiency in fluctuating light. This finding underscores the potential of accelerating quenching relaxation as a building block for improving photosynthetic efficiency in the field. Additionally, by overexpressing natural KEA3 variants with modification to the C-terminus, we show that KEA3 activity is regulated by a mechanism involving its lumen-localized C-terminus, which lowers KEA3 activity in high light. This regulatory mechanism fine-tunes the balance between photoprotective energy dissipation in high light and maximum quantum yield in low light, likely to be critical for efficient photosynthesis in fluctuating light conditions.

Keywords: Arabidopsis • KEA3 • Non-photochemical quenching • PSII quantum efficiency • Thylakoid membrane

Abbreviations: CPA2 domain, cation proton antiport 2 domain; cTP, chloroplast transit peptide; GFP, green fluorescent protein; KEA3, K^+ efflux antiporter 3; KTN domain, K^+ nucleotide-binding domain; NPQ, non-photochemical quenching; qE, energy-dependent quenching; RNA-seq, RNA sequencing.

The nucleotide sequence of KEA3.3 presented in this paper has been submitted to GenBank under accession number KT581346.

Introduction

Sunlight drives plant growth and reproduction through photosynthesis. A large fraction of crop photosynthesis occurs in dense canopy structures, where light availability can undergo massive fluctuations on a short time scale. In such environments, photosynthetic efficiency is tightly linked to the speed with which plant cells can transition between photoprotection in excess light, and high quantum yield in limiting light periods (Murchie and Niyogi 2011, Demmig-Adams et al. 2012). In high light, non-photochemical quenching (NPQ) mechanisms, which dissipate excess absorbed light energy harmlessly as heat and thereby prevent photo-oxidative stress, are rapidly switched on (Müller et al. 2001). However, upon shifts to low light, these mechanisms are not instantly switched off, and the lag in their response time has been hypothesized to limit photosynthetic efficiency in crop canopies (Zhu et al. 2004, Zhu et al. 2010, Long et al. 2015).

Energy-dependent quenching (qE) is the major NPQ mechanism in plants (Demmig-Adams et al. 1996) and contributes significantly to plant fitness in fluctuating light and in the field (Külheim et al. 2002). The qE pathway is activated by a high proton concentration in the thylakoid lumen in periods of excess light, when proton translocation into the lumen by the photosynthetic electron transport chain exceeds proton consumption by ATP synthase (Horton et al. 1996). By dissipating excess absorbed light energy as heat, qE adjusts light energy input into photosynthesis to match the activity of downstream processes. Because qE is proportional to the proton concentration in the lumen, its relaxation kinetics upon transition to low light follow the kinetics of luminal pH decay (Zaks et al. 2012). We recently showed that proton export from the lumen via the thylakoid K^+/H^+ antiporter KEA3 (K^+ efflux antiporter 3) accelerates NPQ relaxation after a high light to low light transition in *Arabidopsis thaliana* (Armbruster et al. 2014). Thereby, KEA3 increases the light efficiency of photosynthesis in fluctuating light.

Here, we show that overexpression of the Arabidopsis major leaf KEA3 isoform (KEA3.2) further accelerates NPQ relaxation in

KEA3.2 and KEA3.1 could be found in the leaf transcriptome in ratios similar to those in the leaf transcriptome obtained from the drought stress experiment (Fig. 1D), suggesting that the minor KEA3 variants are also translated into their respective protein isoforms. The three KEA3 protein isoforms all contain the chloroplast transit peptide (cTP) and the cation/proton antiporter 2 (CPA2) domain, which mediates the K^+/H^+ antiporter. However, the three isoforms differ with respect to their C-termini. The C-terminus of the major KEA3 isoform KEA3.2 contains a putative regulatory K^+ transport, nucleotide-binding (KTN) domain. The KEA3.1-specific splicing event results in a truncated KTN domain with a KEA3.1-specific modification to the C-terminus, whereas the KEA3.3-specific splicing event leads to the production of a truncated protein that lacks the entire C-terminus including the KTN domain (Fig. 1A, E).

Overexpression of KEA3.2 increases PSII quantum efficiency after transition from high to low light

We have previously shown that loss of thylakoid K^+/H^+ antiporter in *kea3* knockout mutants resulted in an increased and extended transient NPQ after transition from the dark-acclimated state to low light conditions and slower NPQ relaxation kinetics after transition from high to low light (Armbruster et al. 2014). This strongly suggested that both the extent of the transient NPQ and NPQ relaxation kinetics are dependent on thylakoid K^+/H^+ antiporter activity and therefore the abundance of KEA3. In order to test whether increasing KEA3 levels can lower the transient NPQ and accelerate NPQ relaxation kinetics, we selected plants that overexpressed a C-terminal green fluorescent protein (GFP)-tagged version of the main KEA3.2 isoform, which had been shown to complement the *kea3-1* NPQ phenotype when expressed at wild-type levels (Armbruster et al. 2014). Out of 100 plants expressing the selection marker, five overexpressed KEA3 protein as compared with Col-0. The two T_2 lines with the highest KEA3.2 expression (six and eight times more as compared with native KEA3 in Col-0, *oeKEA3.2*, Supplementary Fig. S1A) were analyzed for Chl fluorescence after dark acclimation during a time course of low light (10 min at $70 \mu\text{mol photons m}^{-2} \text{s}^{-1}$), high light (5 min at $700 \mu\text{mol photons m}^{-2} \text{s}^{-1}$) and low light (5 min at $70 \mu\text{mol photons m}^{-2} \text{s}^{-1}$), and NPQ was calculated. As we had hypothesized, the *oeKEA3.2* lines displayed a phenotype opposite to that of *kea3-1*, with both a decrease in the transient NPQ after transition from dark to low light (Fig. 2A) and accelerated NPQ relaxation kinetics after transition from high to low light, as compared with the Col-0 wild type (Fig. 2A). In addition, NPQ levels of *oeKEA3.2* stayed below those in Col-0 at the end of the second low light treatment (Fig. 2A). In order to understand whether the lower NPQ in *oeKEA3.2* has a beneficial effect on quantum yield of photosynthesis, we calculated PSII quantum efficiency (Φ_{II}) from the Chl *a* fluorescence data. This analysis demonstrated that PSII quantum efficiency was increased in *oeKEA3.2* as compared with Col-0 between 40 and 80 s after the transition from dark to low light (Supplementary Fig. S2). Also after the high to low light shift, PSII quantum efficiency was significantly higher in

oeKEA3.2 as compared with Col-0 for approximately 40 s after the light intensity shift [$P < 0.001$ at 20 s: +7.6% for *oeKEA3.2* #1 and +9.0% for *oeKEA3.2* #2; $P = 0.02$ at 40 s: +4.8% for *oeKEA3.2* #1 and +6.1% for *oeKEA3.2* #2 at 40 s; one-way analysis of variance (ANOVA) with Tukey's post-hoc test; Fig. 2B; Supplementary Fig. S2]. After 60 s in low light, no significant differences in Φ_{II} could be observed for both *oeKEA3.2* lines.

The transiently higher Φ_{II} in *oeKEA3.2* as compared with the Col-0 could result in higher levels of CO_2 fixation if electrons from H_2O were transported to NADP^+ . However, they could alternatively be transported to O_2 via the Mehler reaction, which would lead to an increase in the production of H_2O_2 (reviewed by Asada 1999). Therefore, we analyzed H_2O_2 levels in Col-0 and *oeKEA3.2* 20 s after shift from high to low light. This analysis showed that at this time point, H_2O_2 levels were slightly, but not significantly higher in *oeKEA3.2* (+ 1.5% as compared with Col-0, Supplementary Fig. S3).

Thylakoid K^+/H^+ antiporter activity is regulated by the KEA3 C-terminus

The observation that NPQ in high light does not markedly respond to KEA3 levels, with *kea3-1* and *oeKEA3.2* showing NPQ values similar to Col-0 (Fig. 2A), suggested that either KEA3 activity does not affect NPQ in high light or that KEA3 is inactive. Because the major KEA3.2 isoform contains a putative regulatory domain at its C-terminus, we decided to analyze the effect of changes to the C-terminus on KEA3 activity. Here, we chose to employ *kea3-1* mutants overexpressing the two minor KEA3 isoforms, KEA3.1 and KEA3.3, which contain a modification to the C-terminus or completely lack the C-terminus, respectively (Fig. 1A, E). For *oeKEA3.1*, we screened 50 plants that expressed the selection marker, and could identify only one line that expressed KEA3.1 protein at higher levels in the T_2 generation than the native KEA3.2 levels in Col-0 (*oeKEA3.1*, Supplementary Fig. S1B). This line expressed KEA3 at about 1.7 times the levels of KEA3 in Col-0, which is four times lower than the levels of KEA3 in the *oeKEA3.2* lines. For KEA3.3, of which all KEA3-expressing lines displayed very high KEA3 levels, we selected T_2 lines with expression levels similar to *oeKEA3.2* (nine and 11 times more as compared with native KEA3 in Col-0, *oeKEA3.3*, Supplementary Fig. S1C). We monitored Chl fluorescence in *oeKEA3.1* and *oeKEA3.3* lines under the same low light, high light regime as for *oeKEA3.2* and calculated NPQ. Interestingly, overexpression of KEA3.1 only partially rescued the *kea3-1* NPQ and PSII quantum efficiency phenotype [while KEA3.2 expressed at wild-type levels fully restored the *kea3-1* NPQ and PSII quantum efficiency phenotype (Armbruster et al. 2014)], suggesting that KEA3.1-GFP is a KEA3 version with intrinsically lower K^+/H^+ antiporter activity (Fig. 2C, D). *oeKEA3.3*, in contrast to *oeKEA3.2*, displayed significantly lower NPQ during the entire high light period, suggesting that KEA3.3, but not KEA3.2, is active in high light (Fig. 2E). No significant difference in PSII quantum yield was detectable between *oeKEA3.3* and Col-0 after transition from high to low light (Fig. 2F; Supplementary Fig. S2C). To analyze whether the specific differences in NPQ and PSII

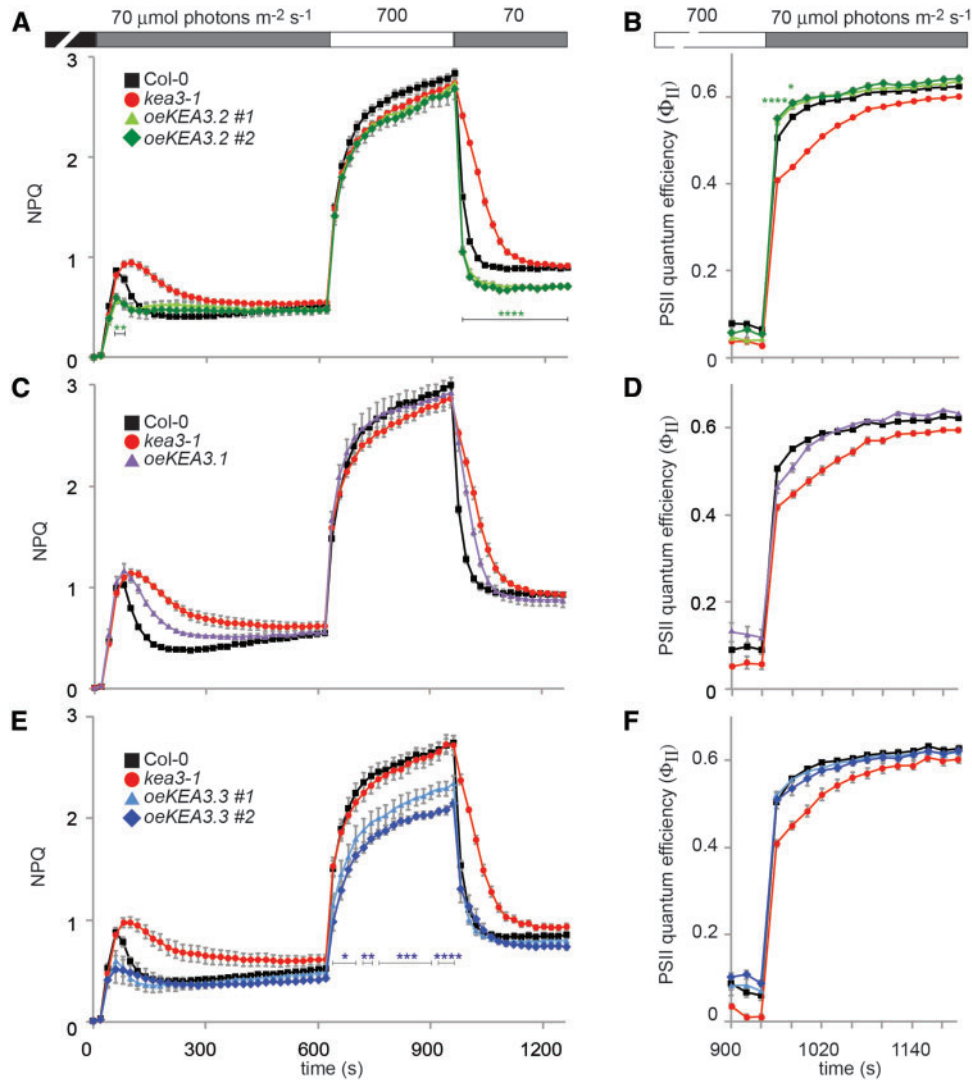


Fig. 2 Overexpression of the different KEA3 splice forms reveals isoform-specific properties. Chl fluorescence of detached, dark-acclimated leaves from Col-0, *kea3-1* and *kea3-1* overexpressing KEA3.2-GFP (*oeKEA3.2*) (A, B), KEA3.1-GFP (*oeKEA3.1*) (C, D) and KEA3.3-GFP (*oeKEA3.3*) (E, F) was monitored during alternating low light (70 $\mu\text{mol photons m}^{-2} \text{s}^{-1}$, gray bar), high light (700 $\mu\text{mol photons m}^{-2} \text{s}^{-1}$, white bar) and low light. NPQ (A, C, E) and PSII quantum efficiency (B, D, F) were calculated. Asterisks indicate where NPQ is significantly lower and PSII quantum efficiency is significantly higher in all the measured lines of one construct as compared with Col-0 (* $0.01 < P < 0.05$; ** $0.005 < P < 0.01$, *** $0.001 < P < 0.005$; **** $P < 0.001$, one-way ANOVA with Tukey post-hoc test). Error bars represent the SEM ($n = 4-6$).

quantum yield between Col-0 and overexpressors of KEA3.2 and KEA3.3 could be due to alterations in the photosynthetic apparatus, we examined Chl content and complex composition and abundance by blue-native (BN)-PAGE. This analysis showed no differences between Col-0 and the KEA3 overexpressors (Supplementary Fig. S4).

Loss of KEA3 results in reduced growth upon a shift to fluctuating light

In order to analyze the effects of KEA3 activity and regulation on plant photosynthesis and growth in fluctuating light, we shifted constant light (150 $\mu\text{mol photons m}^{-2} \text{s}^{-1}$) grown Col-0, *kea3-1*, *oeKEA3.2* and *oeKEA3.3*, which had very similar rosette sizes (Fig. 3A), to alternating high and low light conditions (1 min at 900 $\mu\text{mol photons m}^{-2} \text{s}^{-1}$, 4 min at

90 $\mu\text{mol photons m}^{-2} \text{s}^{-1}$). We then calculated the growth rate during the fluctuating light treatment from increases in leaf area. Due to a much higher variance in *oeKEA3.2* than in the other three genotypes (Fig. 3B), the data failed the ANOVA equal variance test. When we excluded *oeKEA3.2* from the statistical analysis, the growth rate of *kea3-1* was calculated to be significantly smaller as compared with Col-0 ($P = 0.027$, one-way ANOVA with Tukey's posthoc test; Fig. 3A, B; Supplementary Fig. S5).

The KEA3.2 C-terminus is localized in the thylakoid lumen

In order to identify the localization of the KEA3.2 C-terminus, we treated intact thylakoids of KEA3.2-GFP with thermolysin to digest protein regions exposed to the stroma. Addition of the

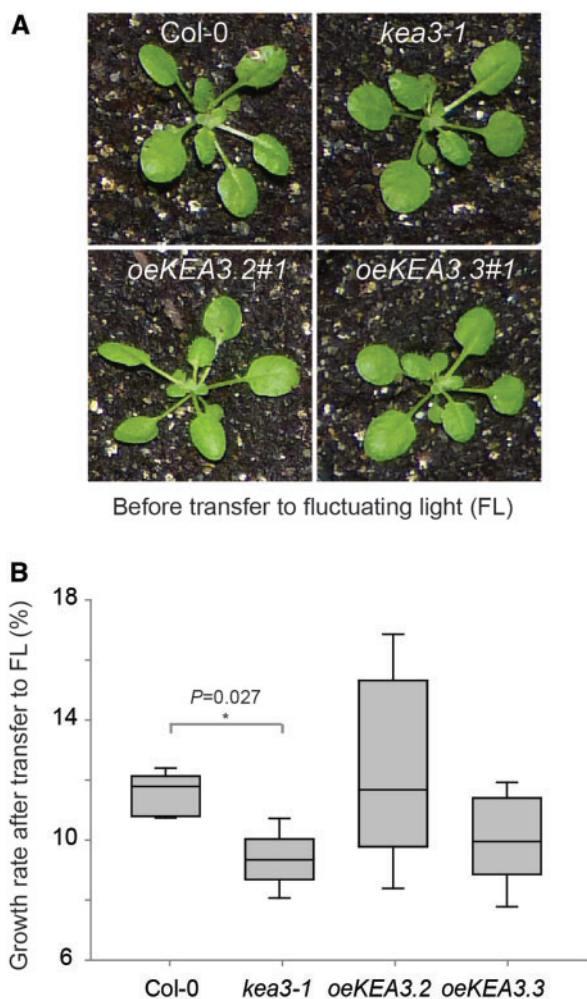


Fig. 3 Loss of KEA3 results in reduced growth upon a shift to fluctuating light. (A) Four-week-old Col-0, *kea3-1*, *oeKEA3.2#1* and *oeKEA3.3#1* before shift to fluctuating high and low light conditions (1 min at $900 \mu\text{mol photons m}^{-2} \text{s}^{-1}$, 5 min at $90 \mu\text{mol photons m}^{-2} \text{s}^{-1}$). (B) Box plot depicting growth rates of Col-0, *kea3-1*, *oeKEA3.2#1* and *oeKEA3.3#1* in fluctuating light as determined by exponential fitting of increases in leaf area over time ($n = 6$; an asterisk indicates a significant difference with $P = 0.027$, excluding *oeKEA3.2*; one-way ANOVA with Tukey post-hoc test). Error bars represent the SEM between measurements.

protease to thylakoids caused detectable KEA3 to shift quantitatively from approximately 100 kDa to approximately 60 kDa, suggesting that the C-terminus, which bears the antibody-binding site, was protected from the protease. In order to investigate whether the protection was caused by the luminal localization of the C-terminus, thylakoids were treated with low concentrations of the detergent Triton X-100 (Fig. 4A), which make the lumen accessible for the protease but do not impact protein–protein interactions (Brooks et al. 2013). After treatment with Triton X-100 and access of thermolysin to the lumen, very little KEA3 could be detected (Fig. 4A). The luminal PSII subunit PsbO was immunodetected as a control for the integrity of the thylakoid membranes. PsbO levels remained largely unchanged by thermolysin treatment, except for when

the thylakoid membrane was disrupted by detergent treatment (Fig. 4A). These experimental data strongly suggest that the KEA3 C-terminus is localized in the thylakoid lumen. This finding was corroborated by in silico thermolysin digestion of a KEA3.2–GFP topology with the luminal C-terminus, which predicted a protected digestion product of 61 kDa detectable with the specific KEA3 antibody (Fig. 4B). The localization of the entire C-terminus to the thylakoid lumen was confirmed by protease treatment of *oeKEA3.3-GFP* thylakoids (Supplementary Fig. S6). In Fig. 4C, a model of the light-dependent regulation of KEA3 activity involving the luminal C-terminus is shown.

Overexpression of AtKEA3 can enhance photosynthetic efficiency in tobacco in fluctuating light

Crop plants experience high fluctuations in light energy availability, especially in their canopies. Because overexpression of KEA3.2 can transiently increase PSII quantum efficiency in Arabidopsis after a high to low light transition, we wanted to test whether the same was true for overexpression of Arabidopsis KEA3.2 (*AtKEA3.2*) in canopy-forming plants. Here we used *Nicotiana benthamiana* (tobacco), which can be transformed transiently with high efficiency (Sainsbury and Lomonosoff 2008) and is from the same genus as the tobacco crop plant *Nicotiana tabacum*. Expression from the 35S promoter of *AtKEA3.2-GFP* and *AtKEA3.3-GFP* in tobacco yielded very similar NPQ results to Arabidopsis (Fig. 5). In high light, *AtKEA3.3-GFP*-expressing leaf sections had low NPQ, whereas sections expressing *AtKEA3.2-GFP* were indistinguishable from the control (Fig. 5A, C). However, upon transition from high to low light, sections expressing either of the two *AtKEA3* isoforms had significantly lower NPQ than the control (Fig. 5A, D). These data suggest that the signal(s) and potential transduction machinery that regulate KEA3 activity are conserved between Arabidopsis and tobacco. We then set out to test whether tobacco sections expressing *AtKEA3.2-GFP* would show repetitive higher PSII quantum efficiencies in fluctuating light conditions. Strikingly, sections expressing *AtKEA3.2-GFP* showed faster NPQ relaxation and higher PSII quantum efficiencies in each low light period of the fluctuating light (Fig. 6A–D; Supplementary Fig. S7).

Discussion

The three different KEA3 isoforms have distinct properties

Analysis of alternative splicing events at the KEA3 locus revealed that the KEA3 genomic DNA encodes at least three different protein isoforms. In the tested conditions, KEA3.2 is clearly the major splice form. This is in line with earlier work, which had shown that KEA3.2 is the only KEA3 protein isoform detectable in leaves (Armbruster et al. 2014). However, KEA3.1 and KEA3.3 are functional K^+/H^+ transporters as seen by their

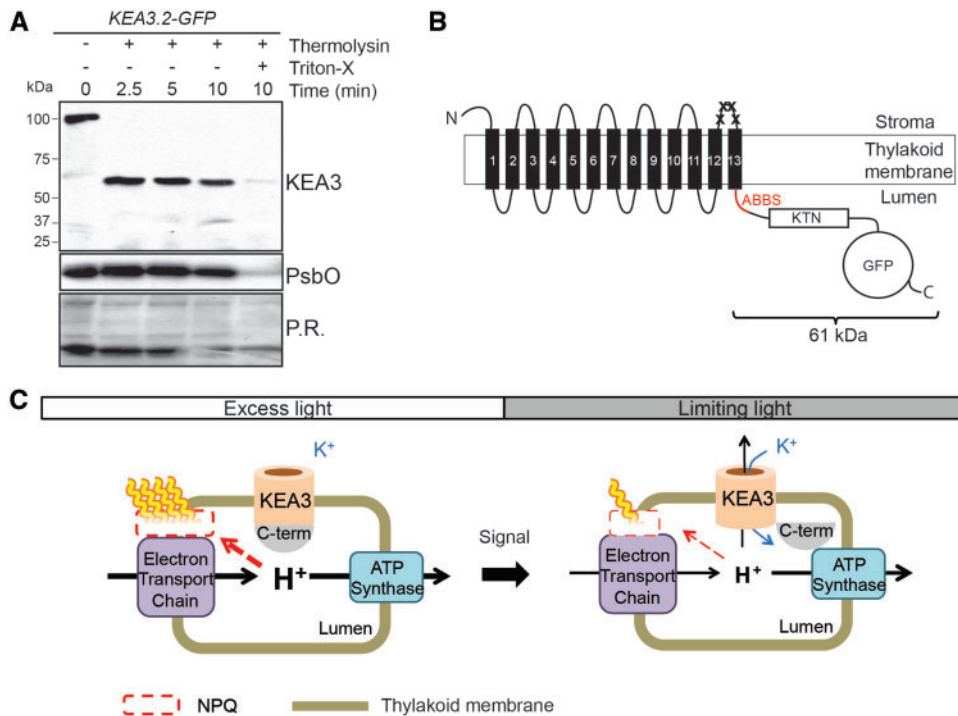


Fig. 4 The KEA3 C-terminus is localized in the thylakoid lumen. (A) Intact thylakoids of *oeKEA3.2* were treated with thermolysin in the absence and presence of Triton X-100. Aliquots were removed at the specified time points, separated by SDS–PAGE, and immunodetection of KEA3 and PsbO was performed. Prior to immunodetection, membranes were stained with Ponceau Red (P.R.). (B) Schematic overview of the KEA3 topology resulting from the thermolysin treatment. The antibody-binding site (ABBS, red, containing five thermolysin sites) present in the C-terminus is protected from thermolysin treatment. Crosses mark stroma-accessible thermolysin sites between transmembrane helices 12 and 13 close to the antibody-binding site. In order to generate this topology model, transmembrane helices of KEA3 were predicted by Phyre2 (see the Materials and Methods). (C) Possible model of light-responsive regulation of KEA3 via the C-terminus.

effect on NPQ (Fig. 2C, E). They differ from KEA3.2 by abolished regulation (KEA3.3) and potentially decreased activity (KEA3.1). Further analyses may reveal conditions where a specific accumulation of either of these two minor KEA3 isoforms has a physiological function.

Residual NPQ limits photosynthetic efficiency upon transition from high to low light

At least two factors have been proposed to limit photosynthetic efficiency immediately following high to low light transitions: (i) residual NPQ that continues to dissipate absorbed light energy as heat (Zhu et al. 2004); and (ii) an overshoot in sucrose synthesis that drains triose-phosphates from the chloroplast and thereby limits Calvin–Benson cycle activity (Prinsley et al. 1986). By overexpressing KEA3.2, we show that the acceleration of NPQ relaxation results in a faster recovery of higher PSII quantum efficiency (Figs. 2, 6; Supplementary Fig. S7). The increase in PSII quantum efficiency is accompanied by a slight, non-significant increase in the Mehler reaction product H_2O_2 (Supplementary Fig. S3). Thus, it appears possible that at least some of the higher PSII quantum efficiency is translated into a higher overall quantum efficiency of photosynthesis.

Our analysis of plant growth rates in fluctuating light suggested that lack of KEA3 imposes a penalty on plant growth in

such conditions (Fig. 3B). Thus, decreases in PSII quantum efficiency and CO_2 assimilation in *kea3* upon transition from high to low light (Armbruster et al. 2014) may be translated into reduced growth rate in fluctuating light. We could not detect an increase in growth rate of *oeKEA3.2* as compared with Col-0 (Fig. 3B). However, *oeKEA3.2* showed much higher variance compared with the other genotypes, and had the two highest growth rates observed in the experiments. The basis of the high variance awaits further elucidation.

KEA3 activity is regulated in a light intensity-responsive manner

Overexpression of the KEA3.3 isoform, which only consists of the CPA2 domain, causes slow NPQ induction and low levels of NPQ in high light, while overexpression of the major KEA3 isoform KEA3.2, which contains an additional C-terminal extension, results in wild-type-like NPQ induction and levels in high light. Plants overexpressing either of the two isoforms show fast NPQ relaxation kinetics upon transition from high to low light. These findings strongly argue for a regulatory function of the C-terminus by inhibiting K^+/H^+ antiport in high light. Intriguingly, such regulation of thylakoid K^+/H^+ antiport activity may constitute a novel regulatory loop in photosynthesis that increases photosynthetic efficiency in fluctuating light: in high light periods, K^+/H^+ antiport via KEA3.2 is inhibited, which allows the

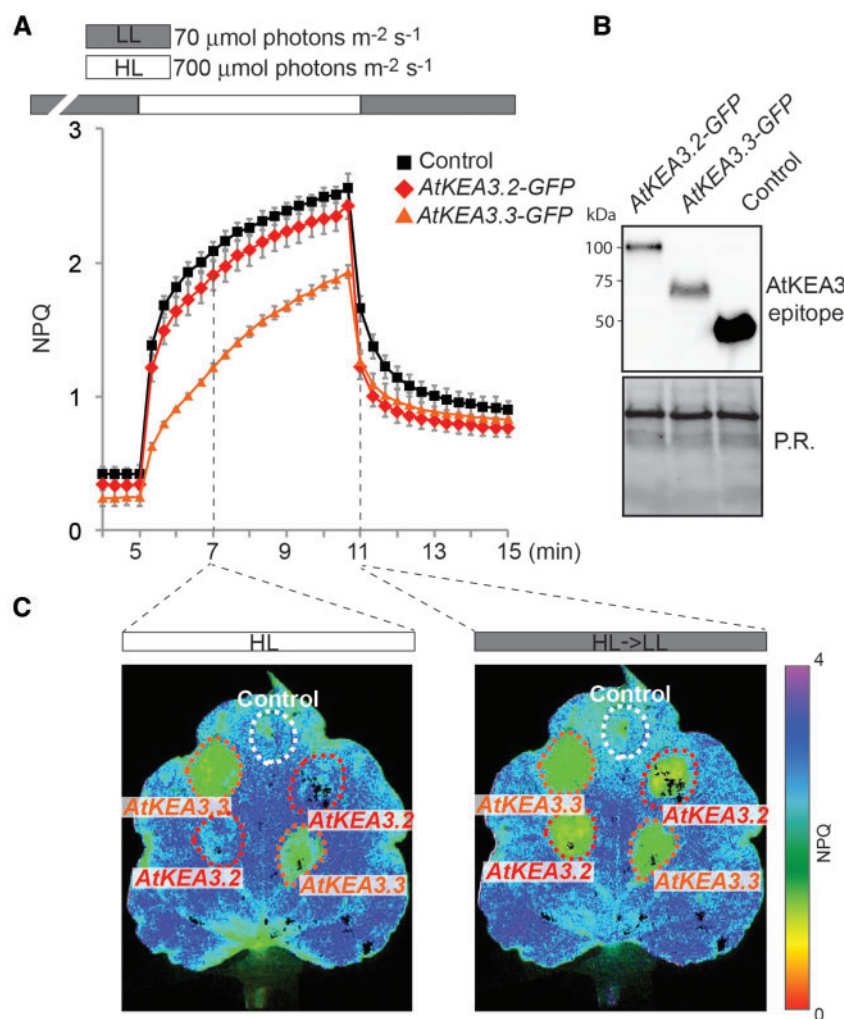


Fig. 5 Overexpression of KEA3.2 and KEA3.3 in tobacco. (A) Chl fluorescence of tobacco leaves transformed with KEA3.2–GFP, KEA3.3–GFP and control (GFP fused to the KEA3 antibody-binding site coding sequence at its N-terminus) was monitored during alternating low light ($70 \mu\text{mol photons m}^{-2} \text{s}^{-1}$, gray bar), high light ($700 \mu\text{mol photons m}^{-2} \text{s}^{-1}$, white bar) and low light. Error bars represent the SEM ($n = 4$). (B) Proteins extracted from the transformed tobacco sections were immunodetected with the specific KEA3 antibody. Ponceau red (P.R.) staining of the membrane prior to immunodetection is shown as a loading control. (C) Images of a tobacco leaf transformed with KEA3.2–GFP, KEA3.3–GFP and control 120 s after transition from low to high light (HL) and 20 s after transition from high to low light (HL→LL 20 s) are shown. False colors represent the NPQ as indicated on the color scheme.

plant to build up a high luminal proton concentration and dissipate excess energy as heat; upon transition to low light, the inhibition is released and the resulting activity of the KEA3 thylakoid K^+/H^+ antiporter facilitates the rapid relaxation of NPQ and recovery of high photosynthetic efficiency (Fig. 4C).

KEA3 activity may be regulated via the C-terminal KTN domain and changes in photosynthetic intermediates

A likely candidate involved in the light intensity-responsive gating of KEA3.2 K^+/H^+ antiport is its C-terminal KTN domain. KTNs (RCKs) are highly conserved protein domains found ubiquitously in prokaryotes and eukaryotes, which regulate K^+ transporters and channels in response to changes in NADH/NAD^+ or ATP/ADP (Roosild et al. 2002, Kröning et al. 2007, Roosild et al. 2009, Cao et al. 2013). Sequence alignments of

KTN domains from Arabidopsis KEA3 and KEA2 (Aranda-Sicilia et al. 2012, Kunz et al. 2014), *Escherichia coli* KefC (Roosild et al. 2009) and *Vibrio parahaemolyticus* TrkA (Cao et al. 2013) show high sequence conservation of the amino acids surrounding and comprising the specific nucleotide-binding site (Supplementary Fig. S8A), suggesting that the KTN domains of KEA3 (and KEA2) also bind nucleotides. The ratios of both nucleotide pairs ATP/ADP and $\text{NADPH}/\text{NADP}^+$ have been shown to decrease in response to a transition from excess light to limiting light conditions (Stitt et al. 1989) and thus might constitute or contribute to the signal that triggers KEA3 activation. Both photosynthetic intermediates are present in the chloroplast stroma, and ATP/ADP has been reported to cross the thylakoid membrane into the lumen (Spetea et al. 2004). The localization of the KEA3.2 C-terminus to the thylakoid lumen suggests that the Rossman fold of the KTN domain binds

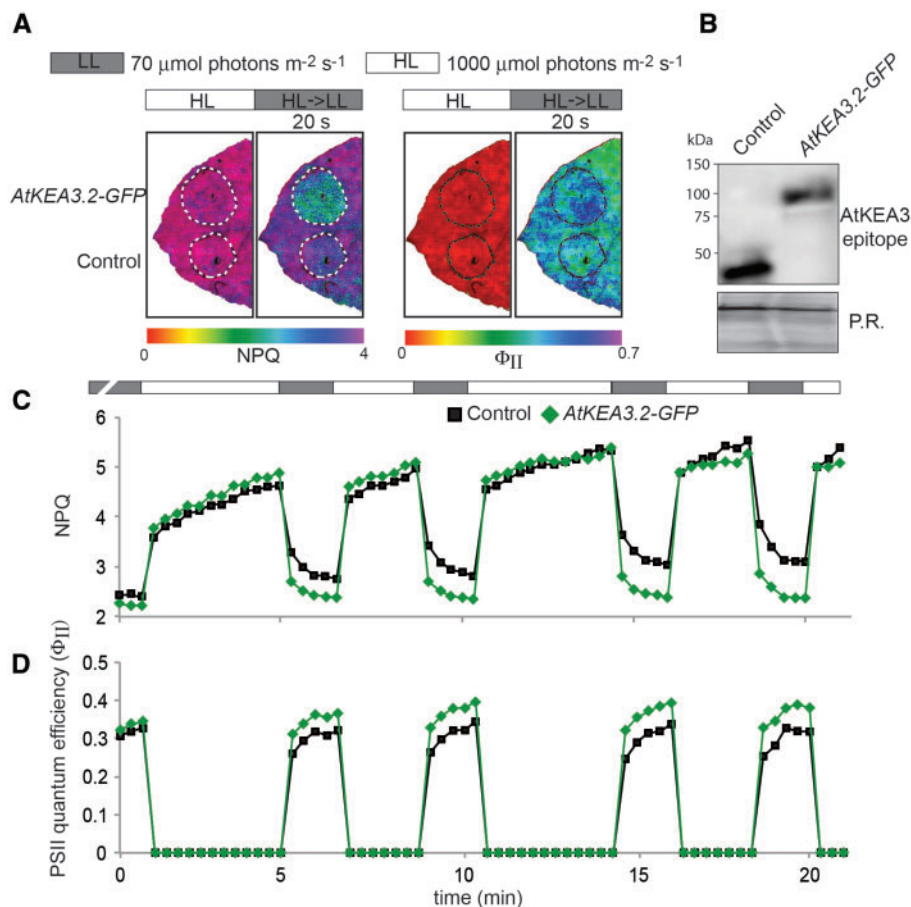


Fig. 6 Overexpression of *KEA3.2* in tobacco enhances PSII quantum yield in fluctuating light. (A) Images of a tobacco leaf transformed with either *KEA3.2-GFP* or *GFP* fused to the *KEA3* antibody-binding site coding sequence at its N-terminus (control) at the end of the high light period (1,000 $\mu\text{mol photons m}^{-2} \text{s}^{-1}$, white bar; HL) and 20 s after transition from high to low light (70 $\mu\text{mol photons m}^{-2} \text{s}^{-1}$, gray bar; HL > LL 20 s). False colors represent the NPQ in the left panel and PSII quantum efficiency in the right panel as indicated by the respective color bars. (B) Immunodetection of proteins extracted from the transformed tobacco sections with the specific *KEA3* antibody. Ponceau red (P.R.) staining of the membrane prior to immunodetection is shown as a loading control. (C, D) Chl fluorescence of tobacco leaves transformed with *KEA3.2-GFP* and control was monitored under fluctuating high light (1,000 $\mu\text{mol photons m}^{-2} \text{s}^{-1}$, white bar) and low light (70 $\mu\text{mol photons m}^{-2} \text{s}^{-1}$, gray bar), and NPQ (C) and PSII quantum efficiency (D) were calculated. Because of the high background variation in PSII quantum efficiency between different tobacco leaves, a representative trace from one experiment is shown. More traces can be found in **Supplementary Fig. S7**.

nucleotides that can enter the thylakoid lumen. According to our current knowledge of luminal nucleotides, these may be either ATP/ADP or GTP/GDP (Spetea *et al.* 2004).

There is ample experimental evidence suggesting that KTN domains gate K^+ fluxes by reversibly interacting with a gating structure of the ion transporter domain (Ness and Booth 1999, Roosild *et al.* 2002). This gating structure is moderately conserved in *KEA3.2* (two out of three potentially critical acidic amino acid residues are conserved; **Supplementary Fig. S8B**). Because *KEA3* is activated within seconds of the transition from high to low light, we propose that *KEA3* regulation is triggered by certain photosynthesis intermediates, the levels of which change in response to excitation energy. Besides ATP/ADP ratios, which may regulate *KEA3* activity via binding to the luminal KTN domain, other photosynthetic intermediates immediately affected by changes in excitation energy include the plastoquinone pool (Stitt *et al.* 1989, Grieco *et al.* 2012) and the electric potential across the thylakoid membrane

(Kramer *et al.* 2003). Because activation of *KEA3* seems to precede large changes in NPQ, and NPQ is proportional to the proton concentration in the lumen, we can probably exclude luminal pH as a potential signal.

Conclusion

Results demonstrating that PSII quantum efficiency can be increased by accelerating NPQ relaxation via overexpression of *KEA3.2* (**Figs. 2A, B, 6**) suggest rapid NPQ relaxation in general and enhancement of *KEA3* activity in particular as promising building blocks for improving photosynthesis in the field. In future, understanding the specific signal(s) and regulatory mechanism that allow *KEA3* activity to respond to changes in light intensity may unravel the molecular basis to an additional feedback loop of photosynthesis involved in optimizing photosynthesis in natural, fluctuating light environments.

Materials and Methods

Identification and expression analysis of alternative KEA3 splice forms

cDNA was synthesized from total leaf RNA using superscript III (Invitrogen) and oligo(dT) primers according to the manufacturer's instruction. Primers specific for the KEA3.2 transcript (Armbruster et al. 2014) were used for amplification and Gateway-mediated recombination into pDONR201. Besides KEA3.2, two further splice forms, KEA3.1 and KEA3.3, were identified in the resulting pDONR201-KEA3 constructs. Large-scale analysis of splice form abundances was performed by filtering publicly available Col-0 RNA-seq data deposited in the sequence read archive (SRA) of NCBI (<http://www.ncbi.nlm.nih.gov/sra>) for the splice form-specific 18-mers TTCCCCGGGGTTATTCTT (KEA3.1), TTCCCCGGGAGTCCTATT (KEA3.2/KEA3.3), CCCGGAGAGGTGAA GATG (KEA3.3), GAGAGAAAATAGGTGAAG (KEA3.1/KEA3.2) and CAGAAAC TCTCCTCTCAA (At3g04780, control).

Plant material, propagation and growth conditions

kea3-1 plants overexpressing the KEA3 variants with a C-terminal GFP tag were generated as described previously (Armbruster et al. 2014). KEA3.1 and KEA3.3 cDNA sequences were amplified using the same forward primer as for KEA3.2, and 5'-GGGGACCACTTTGTACAAGAAAGCTGGGTTAACGATTTTATTGA CAAAA-3' (KEA3.1) and 5'-GGGGACCACTTTGTACAAGAAAGCTGGGTCATCTT CACTCTCCGGAT-3' (KEA3.3), and introduced into pB7FWG2 (Karimi et al. 2002).

Col-0, *kea3-1* and *kea3-1* plants overexpressing KEA3.1-GFP, KEA3.2-GFP and KEA3.3-GFP were grown on Sunshine Mix 4 potting mix (Sun Gro Horticulture Distribution) in controlled conditions of 10 h dark, 22 °C/14 h light, 23 °C, with a light intensity of 120 μmol photons m⁻² s⁻¹.

For fluctuating light experiments, plants were grown for 4 weeks in controlled short-day conditions of 8 h light, 20 °C/16 h dark, 16 °C, with a light intensity of 150 μmol photons m⁻² s⁻¹ and then shifted to alternating high and low light (1 min at 900 μmol photons m⁻² s⁻¹, 4 min at 90 μmol photons m⁻² s⁻¹) in the short-day light period for 6 d. Leaf area of whole plants was determined by using ImageJ. Growth rates were determined by exponential fitting.

Transient expression of KEA3 isoforms in *Nicotiana benthamiana*

For use as a control, a KEA3 fragment containing the KEA3 antibody-binding site was fused to the N-terminus of GFP, employing the primers 5'-GGGGACAA GTTTGTACAAAAAGCAGGCTATGAACCAACTTGAAGAAAAGccg-3' and 5'-GGGGACCACTTTGTGAAAGCTGGGTTTGCATCTGTGGCTCCTGCTTT-3', and introduction of the amplified region into pB7FWG2 (Karimi et al. 2002). Colonies of *Agrobacterium tumefaciens* strain GV3101 transformed with the KEA3-GFP constructs or the control were resuspended in induction medium (0.1 mM MES pH5.6, 0.1 mM MgCl₂, 0.1 mM acetosyringone) to an OD₆₀₀ of 0.5. After 2 h at 28 °C, suspensions were inoculated onto sections of *N. benthamiana* (tobacco) leaves. Transfected plants were grown for 2–3 d in room light before detached leaves were scored for Chl fluorescence.

Chl fluorescence and H₂O₂ measurements

For NPQ and Φ_{II} measurements, detached leaves of 5-week-old Arabidopsis plants were placed onto wet filter paper. Detached leaves of tobacco were placed with their petioles in centrifuge tubes containing water and sealed with parafilm. Leaves were dark acclimated for 30 min prior to measurement. Room temperature Chl *a* fluorescence of these leaves was monitored using the Walz MAXI IMAGING-PAM with blue actinic LEDs set to approximately 70 and 700/1,000 μmol photons m⁻² s⁻¹ (low and high light, respectively). To measure *F_m* and *F_m'*, white light pulses (4,000 μmol photons m⁻² s⁻¹, duration 0.8 s) were applied. NPQ was calculated as (*F_m* - *F_m'*)/*F_m'* and Φ_{II} as (*F_m'* - *F_s*)/*F_m'*. For H₂O₂ measurements, leaves were rapidly frozen 20 s after transition from high to low light employing the Imaging PAM as light source with the same program used for the NPQ and Φ_{II} measurements. Hydrogen peroxide was detected by resorufin (Strand et al. 2015). In detail, leaves were ground in liquid nitrogen and extracted

in 50 mM potassium phosphate buffer (pH 7.5). Extracts were incubated in a reaction buffer containing 10 U ml⁻¹ horseradish peroxidase (Sigma) and 5 μM Amplex Red (Invitrogen) for 30 min in the dark. Peroxide concentration of the sample was estimated by comparison with a standard curve and relative to Chl. Depicted values were calculated by normalizing to the Col-0 average. Chl content was determined according to Porra et al. (1989).

For *F_v*/*F_m* [(*F_m* - *F₀*)/*F_m*] measurements, whole plants were dark acclimated for 30–45 min prior to measurement with the Walz MAXI IMAGING-PAM. *F_v*/*F_m* values are averages of the whole plant. *F_v*/*F_m* recovery for each plant was measured as the *F_v*/*F_m* ratio after 6 d in fluctuating light and *F_v*/*F_m* before shift.

Statistical analyses on data were performed by employing one-way ANOVA and Tukey's multiple comparison tests.

Protease protection assay, immunoblot analyses and BN-PAGE

Thylakoids were isolated as described (Armbruster et al. 2014). For protease protection assays, thylakoids were resuspended at 0.5 mg Chl per ml⁻¹ in 0.3 M sorbitol, 2.5 mM EDTA, 5 mM MgCl₂, 0.5% (w/v) bovine serum albumin (BSA), 20 mM HEPES (pH 7.6). Reactions were started by the addition of thermolysin (EMD Millipore) at 10 μg ml⁻¹ to a final volume of 300 μl. At the indicated times, the reaction was stopped by transferring 50 μl to a tube containing EDTA so that the final concentration of EDTA was 50 mM. The tubes were vortexed immediately and sample buffer was added. For BN-PAGE, thylakoid membranes were solubilized with 0.7% β-*n*-dodecyl-d-maltoside (w/v) and separated by BN gels (Invitrogen) according to Peng et al. (2008).

Total protein was extracted from liquid nitrogen frozen leaf tissue (20 mg) supplemented with approximately 50 μl of lysing matrix D (MP Biomedicals). The Fastprep 24 tissue homogenizer (MP Biomedicals) was set to 6.5 s⁻¹ and tissue was disrupted for 1 min prior to addition of 200 μl of protein extraction buffer [200 mM Tris, pH 6.8, 8% SDS (w/v), 40% glycerol and 200 mM dithiothreitol (DTT)]. Samples were heated at 65 °C for 10 min and proteins were separated on SDS-PAGE, blotted onto nitrocellulose, visualized with Ponceau Red [0.1% Ponceau S (w/v) in 5% (v/v) acetic acid] and detected with antibodies specific for KEA3 (Armbruster et al. 2014) or PsbO (Agrisera). KEA3 signals were quantified by densitometric analysis of Western bands and Ponceau stain using NIH ImageJ software and associated plug-ins (<http://imagej.nih.gov/ij/>).

Computational analyses

Arabidopsis KEA3.1 and KEA3.2 (At4g04850.1 and At4g04850.2) DNA and protein sequences were retrieved from TAIR (The Arabidopsis Information Resource; www.arabidopsis.org). The newly identified KEA3.3 splice form was translated into protein sequence by using ExPASy Translate (web.expasy.org/translate). Amino acid sequences were aligned using ClustalOmega (<http://www.ebi.ac.uk/Tools/msa/clustalo>). Transmembrane helices of KEA3 were predicted by homology modeling using the Phyre2 server (www.sbg.bio.ic.ac.uk/~phyre2; Kelley and Sternberg 2009). Thermolysin digestion sites were predicted with ExPASy Peptide Cutter (web.expasy.org/peptide_cutter). For sequence comparisons, sequences of the KTN domain of *E. coli* KefC (EckefC, P03819), AtKEA3, Arabidopsis KEA2 (AtKEA2, Q65272) and the first RCK domain of *V. parahaemolyticus* TrkA (VcTrkA, A0A072LGS4) were aligned using ClustalOmega and shaded according to amino acid identity (black) and similarity (gray) using the Box-shade server (http://www.ch.embnet.org/software/BOX_form.html).

Accession numbers

Sequence data determined for the KEA3.3 cDNA have been submitted to GenBank under accession number KT581346. Accession numbers for RNA-seq data used in this analysis were SRR656215, SRR656216, SRR656217, SRR656218; ERR754059, ERR754064, ERR754066, ERR754069, ERR754077, ERR754084, ERR754087 (Clauw et al. 2015) and ERR377676, ERR377677, ERR377678 (Aubry et al. 2014).

Supplementary data

Supplementary data are available at PCP online

Funding

This work was supported by the Carnegie Institution for Science; the Max Planck Society; the Bill & Melinda Gates Foundation RIPE project at the University of Illinois [a subaward]; the Howard Hughes Medical Institute; the Gordon and Betty Moore Foundation [grant GBMF3070 to K.K.N.]; the Deutsche Forschungsgemeinschaft [AR 808/1-1, 1-2 to U.A.].

Acknowledgements

We thank Elisabeth Schmidtman for excellent technical assistance, Mark Aurel Schöttler and Ralph Bock for help with the fluctuating light chamber, and anonymous reviewers for constructive comments and suggestions.

Disclosures

The Carnegie Institution for Science has submitted a patent form on behalf of U.A., M.C.J. and K.K.N. on aspects of the finding.

References

- Aranda-Sicilia, M.N., Cagnac, O., Chanroj, S., Sze, H., Rodriguez-Rosales, M.P. and Venema, K. (2012) Arabidopsis KEA2, a homolog of bacterial KefC, encodes a K(+)/H(+) antiporter with a chloroplast transit peptide. *Biochim. Biophys. Acta* 1818: 2362–2371.
- Armbruster, U., Carrillo, L.R., Venema, K., Pavlovic, L., Schmidtman, E., Kornfeld, A., et al. (2014) Ion antiport accelerates photosynthetic acclimation in fluctuating light environments. *Nat. Commun.* 5: 5439.
- Asada, K. (1999) The water–water cycle in chloroplasts: scavenging of active oxygens and dissipation of excess photons. *Annu. Rev. Plant Physiol. Plant Mol. Biol.* 50: 601–639.
- Aubry, S., Smith-Unna, R.D., Bournnell, C.M., Kopriva, S. and Hibberd, J.M. (2014) Transcript residency on ribosomes reveals a key role for the Arabidopsis thaliana bundle sheath in sulfur and glucosinolate metabolism. *Plant J.* 78: 659–673.
- Brooks, M.D., Sylak-Glassman, E.J., Fleming, G.R. and Niyogi, K.K. (2013) A thioredoxin-like/beta-propeller protein maintains the efficiency of light harvesting in Arabidopsis. *Proc. Natl. Acad. Sci. USA* 110: E2733–E2740.
- Cao, Y., Pan, Y., Huang, H., Jin, X., Levin, E.J., Kloss, B., et al. (2013) Gating of the TrkH ion channel by its associated RCK protein TrkA. *Nature* 496: 317–322.
- Clauw, P., Coppens, F., De Beuf, K., Dhondt, S., Van Daele, T., Maleux, K., et al. (2015) Leaf responses to mild drought stress in natural variants of Arabidopsis. *Plant Physiol.* 167: 800–816.
- Demmig-Adams, B., Adams, W.W., III, Barker, D.H., Logan, B.A., Bowling, D.R. and Verhoeven, A.S. (1996) Using chlorophyll fluorescence to assess the fraction of absorbed light allocated to thermal dissipation of excess excitation. *Physiol. Plant.* 98: 253–264.
- Demmig-Adams, B., Cohu, C.M., Muller, O. and Adams, W.W., 3rd (2012) Modulation of photosynthetic energy conversion efficiency in nature: from s to seasons. *Photosynth. Res.* 113: 75–88.
- Grieco, M., Tikkanen, M., Paakkarinen, V., Kangasjarvi, S. and Aro, E.M. (2012) Steady-state phosphorylation of light-harvesting complex II proteins preserves photosystem I under fluctuating white light. *Plant Physiol.* 160: 1896–1910.
- Horton, P., Ruban, A.V. and Walters, R.G. (1996) Regulation of light harvesting in green plants. *Annu. Rev. Plant Physiol. Plant Mol. Biol.* 47: 655–684.
- Karimi, M., Inze, D. and Depicker, A. (2002) GATEWAY vectors for Agrobacterium-mediated plant transformation. *Trends Plant Sci.* 7: 193–195.
- Kelley, L.A. and Sternberg, M.J. (2009) Protein structure prediction on the Web: a case study using the Phyre server. *Nat. Protoc.* 4: 363–371.
- Kramer, D.M., Cruz, J.A. and Kanazawa, A. (2003) Balancing the central roles of the thylakoid proton gradient. *Trends Plant Sci.* 8: 27–32.
- Kröning, N., Willenborg, M., Tholema, N., Hanelt, I., Schmid, R. and Bakker, E.P. (2007) ATP binding to the KTN/RCK subunit KtrA from the K⁺-uptake system KtrAB of *Vibrio alginolyticus*: its role in the formation of the KtrAB complex and its requirement in vivo. *J. Biol. Chem.* 282: 14018–14027.
- Külheim, C., Agren, J. and Jansson, S. (2002) Rapid regulation of light harvesting and plant fitness in the field. *Science* 297: 91–93.
- Kunz, H.H., Gierth, M., Herdean, A., Satoh-Cruz, M., Kramer, D.M., Spetea, C., et al. (2014) Plastidial transporters KEA1, -2, and -3 are essential for chloroplast osmoregulation, integrity, and pH regulation in Arabidopsis. *Proc. Natl. Acad. Sci. USA* 111: 7480–7485.
- Long, S.P., Marshall-Colon, A. and Zhu, X.G. (2015) Meeting the global food demand of the future by engineering crop photosynthesis and yield potential. *Cell* 161: 56–66.
- Müller, P., Li, X.P. and Niyogi, K.K. (2001) Non-photochemical quenching. A response to excess light energy. *Plant Physiol.* 125: 1558–1566.
- Murchie, E.H. and Niyogi, K.K. (2011) Manipulation of photoprotection to improve plant photosynthesis. *Plant Physiol.* 155: 86–92.
- Ness, L.S. and Booth, I.R. (1999) Different foci for the regulation of the activity of the KefB and KefC glutathione-gated K⁺ efflux systems. *J. Biol. Chem.* 274: 9524–9530.
- Peng, L., Shimizu, H. and Shikanai, T. (2008) The chloroplast NAD(P)H dehydrogenase complex interacts with photosystem I in Arabidopsis. *J. Biol. Chem.* 283: 34873–34879.
- Porra, R.J., Thompson, W.A. and Kriedemann, P.E. (1989) Determination of accurate extinction coefficients and simultaneous equations for assaying chlorophylls a and b extracted with four different solvents: verification of the concentration of chlorophyll standards by atomic absorption spectroscopy. *Biochim. Biophys. Acta* 975: 384–394.
- Prinsley, R.T., Hunt, S., Smith, A.M. and Leegood, R.C. (1986) The influence of a decrease in irradiance on photosynthetic carbon assimilation in leaves of *Spinacia oleracea* L. *Planta* 167: 414–420.
- Roosild, T.P., Castronovo, S., Miller, S., Li, C., Rasmussen, T., Bartlett, W., et al. (2009) KTN (RCK) domains regulate K⁺ channels and transporters by controlling the dimer-hinge conformation. *Structure* 17: 893–903.
- Roosild, T.P., Miller, S., Booth, I.R. and Choe, S. (2002) A mechanism of regulating transmembrane potassium flux through a ligand-mediated conformational switch. *Cell* 109: 781–791.
- Sainsbury, F. and Lomonosoff, G.P. (2008) Extremely high-level and rapid transient protein production in plants without the use of viral replication. *Plant Physiol.* 148: 1212–1218.
- Spetea, C., Hundal, T., Lundin, B., Heddad, M., Adamska, I. and Andersson, B. (2004) Multiple evidence for nucleotide metabolism in the chloroplast thylakoid lumen. *Proc. Natl. Acad. Sci. USA* 101: 1409–1414.
- Stitt, M., Scheibe, R. and Feil, R. (1989) Response of photosynthetic electron transport and carbon metabolism to a sudden decrease of irradiance in the saturating or the limiting range. *Biochim. Biophys. Acta* 973: 241–249.
- Strand, D.D., Livingston, A.K., Satoh-Cruz, M., Froehlich, J.E., Maurino, V.G. and Kramer, D.M. (2015) Activation of cyclic electron flow by hydrogen peroxide in vivo. *Proc. Natl. Acad. Sci. USA* 112: 5539–5544.

- Zaks, J., Amarnath, K., Kramer, D.M., Niyogi, K.K. and Fleming, G.R. (2012) A kinetic model of rapidly reversible nonphotochemical quenching. *Proc. Natl. Acad. Sci. USA* 109: 15757–15762.
- Zhu, X.G., Long, S.P. and Ort, D.R. (2010) Improving photosynthetic efficiency for greater yield. *Annu. Rev. Plant Biol.* 61: 235–261.

- Zhu, X.G., Ort, D.R., Whitmarsh, J. and Long, S.P. (2004) The slow reversibility of photosystem II thermal energy dissipation on transfer from high to low light may cause large losses in carbon gain by crop canopies: a theoretical analysis. *J. Exp. Bot.* 55: 1167–1175.

